Technical abilities and limitations of acoustic rhinometry optimised for infants*

P.G. Djupesland[1], B. Lyholm[2]

[1] Department of Otorhinolaryngology, Ullevaal University Hospital, 0407, Oslo, Norway
[2] "Numerical Lab", Copenhagen, Denmark

SUMMARY *The objective of this model study was to validate in detail the technical capabilities as well as the limitations of a new rhinometric probe optimised for infants in order to improve reliability of measurements and reduce the risk of misleading conclusions.*
The repeatability was excellent (CV<0.6%) and the reproducibility was high (CV%<4%) provided the ambient conditions were fairly stable. The repeatability declined when external noise levels were above 60 dB SPL, and variation in temperature and pressure reduce reproducibility. The accuracy of the minimum cross-sectional area (MCA) as well as the volume corresponding to the nasal cavity in infants (VOL4), was acceptable (% error <12%) as long as the MCA was larger than 30-40% of the probe dimensions and the cross-sectional area of the cavity posterior to the MCA did not exceed the MCA by a factor of more than 3-4. Variation in the position of the MCA within the anterior 2 cm has minimal influence on the posterior measurements provided the shape and length of the MCA are unaltered. Rods inserted into the tubular model to simulate the slit-like shape of the nasal passage did not reduce the accuracy, which is essential to the clinical value of acoustic rhinometry. Recommendations and guidelines designed to enhance the reliability of acoustic measurements in infants are presented.

Key words: acoustic rhinometry, nasal airway, neonates, reflectrometry, technical properties.

INTRODUCTION

Acoustic reflectrometry was first applied in humans to determine the dimensions and dynamics of the pulmonary and pharyngeal airways (Sondhi and Gopinath, 1970; Jackson et al., 1977; Hoffstein and Fredberg, 1991; Rivlin et al., 1984). Theoretical and practical constraints mainly related to the location and dimensions of these airways have unfortunately so far limited its clinical application (Jackson et al., 1977; Molfino et al., 1990). The smaller dimensions and easy access to the nasal airways, however, reduce these limitations considerably and led to the development of acoustic rhinometry (AR) for adults (Hilberg et al., 1989) and more recently a miniprobe optimised for infants (Djupesland and Lyholm, 1997).

Several recent reports have focused on both technical and practical limitations increasing the risk of artefacts and errors during measurements. Approximations to the theoretical assumptions of acoustic reflectrometry; negligible viscous loss, no (or symmetrical) branching, rigid walls and planar wave propagation represent obvious sources of error, but their impact on actual measurements vary with the properties of the incident sound signal, analysing software, the dimensions and design of the probes and coupling devices applied (Hamilton et al., 1995; Hamilton et al. 1997; Riechelmann et al., 1993; Zavras et al., 1994; Tomkinson, 1995; Marchall, 1992; Lenders et al., 1992; Buenting et al., 1994; Roithmann et al., 1995; Tomkinson and Eccles, 1995; Hilberg et al., 1989; Djupesland and Lyholm, 1997). Overestimation may result from insufficient coupling between the nosepiece and the nostril, large communications to the sinuses (Hilberg and Pedersen, 1996) and expansion of the valve area by conical nosepieces (Fisher and Boreham, 1995; Hilberg et al., 1989; Fisher et al., 1995; Hamilton et al. 1997), while underestimation may result from inappropriate positioning and pressure on the *ala nasi* by anatomical nosepieces (Roithmann et al., 1995). Pressure changes during respiration (Fisher et al., 1995; Roithmann et al., 1995), variation in temperature (Tomkinson and Eccles, 1996) and external noise also represent potential sources of error.

Insufficient awareness of the technical limitations and failure to recognise artefacts may cause misinterpretation of the rhino-

* Received for publication January 16, 1998; accepted July 15, 1998

metric results (Tomkinson, 1997). Nevertheless, validation data are limited, and at present no official guidelines or standards as to validation of rhinometric equipment exist (Tomkinson, 1997). The objective of this model study is, therefore, to validate in detail the technical capabilities as well as the limitations of a new rhinometric probe optimised for infants (Djupesland and Lyholm, 1997).

MATERIAL AND METHODS

Theoretical consideration

The basic principles of acoustic reflectometry (Marchall, 1992; Sondhi and Gopinath, 1970; Fredberg et al., 1980; Jackson et al., 1977), and the particular features of AR for adults (Hilberg et al., 1989) have been reported elsewhere. Some features important to the optimised probe for infants (Djupesland and Lodrup Carlsen, 1997; Djupesland et al., 1997; Djupesland and Lyholm, 1997), will be described in some detail. The ability to measure steep changes, and thereby the ability to resolve small constrictions in the cavity, is defined as the rise distance, i.e. the distance the rhinometer will need to recover from 10% to 90% of the final value of an infinite steep change in the cavity (Hilberg et al., 1998). The rise distance is primarily determined by the acoustic signal bandwidth (f_{max}) (Hilberg et al., 1998) which again is restricted by the methodological requirements of planar wave propagation in the cavity. Assumptions of planar wave propagation are valid as long as the equation [($f_{max}=1.84c_0/\Pi d_{max}$, or simplified $f_{max}=c_0/2d_{max,}$) (c_o= speed of sound in air, d_{max}= maximum diameter in the cavity)] is respected. At frequencies above f_{max} higher-order reflections, or cross-modes, will occur. Taking these considerations into account, and assuming d_{max}=0.8 or CA_{max}=0.5 cm^2 , the upper frequency limit of the miniprobe would theoretically be approximately 24.9 kHz. In practice the speaker, microphone and 44.1 kHz sampling frequency (f_S) have resulted in an effective upper frequency of 20 kHz. The sound pressure is 70 dB SPL. The increased signal bandwidth greatly increases the miniprobe's ability to measure steep changes in the cavity compared to adult probes (Hilberg et al., 1998) (Djupesland, unpublished observations). This seems to be in close agreement with Fredberg et al. (1980) suggestions for estimating the 0-63% rise distance as $c_0/6f_{max}$. The spatial resolution (SR) of the area-distance relationship (AD) curve, defined as the distance between actually measured points in the curve is solely determined by the sampling frequency and the speed of sound since SR= $c_0/\ 2f_S$. Given that the sampling frequency is 44.1 kHz, the distance between points in the AD curve is 3.8 mm. It is important to emphasise that increasing the sampling frequency without increasing the acoustic signal bandwidth, will not in itself improve the measuring capabilities of the probe.

Continuous wide band rhinometry

In the wide-band noise rhinometer, the pulsed analog signal of traditional rhinometers, is replaced by a digital continuous wide-band noise generated by an advanced digital signal processor (DSP) (Djupesland and Lyholm, 1997). In traditional rhinometers, the need to separate impulse responses in the tube limits the rate at which measurements can be made and the absolute theoretical limit is accepted to be 20 per second (Sondhi and Gopinath, 1970). By contrast, the continuous signal and high speed of the DSP of the continuous wide band rhinometer, currently perform approximately 100 measurements per second. A high measuring rate permits implementation of averaging and error rejection algorithms which improve the repeatability, reproducibility and accuracy and is a precondition for future evaluation of upper airway dynamics.

The model

Models consisted of circular metallic disks of 1 or 4 mm thickness which were perforated in the centre by high precision burrs used in advanced mechanical production. The circular holes ranged from 0.02 cm^2 to 0.6 cm^2 to enable reconstruction of cavities with cross-sectional areas and volumes similar to the nasal airway of infants. The discs fitted into a 70 mm deep plastic container which was closed by a tap which held the discs tightly together. By rearranging these discs, cavities with differences in minimum cross-sectional area (MCA), its position, length and shape as well as variation of the posterior part of the cavity could be modelled (Fig. 1). The algorithm used in AR is not valid in case non-symmetrical bifurcation (Jackson et al., 1977; Hilberg et al., 1989) impeding reliable determination of the nasopharynx (Djupesland et al., 1997; Tomkinson, 1997). The effects of the contra-lateral nostril and the common communications to the oropharynx on nasal airway measurements anterior to the bifurcation (Djupesland et al., 1997; Djupesland and Lyholm, 1997) are, however, negligible, justifying the use of a single-tube model.

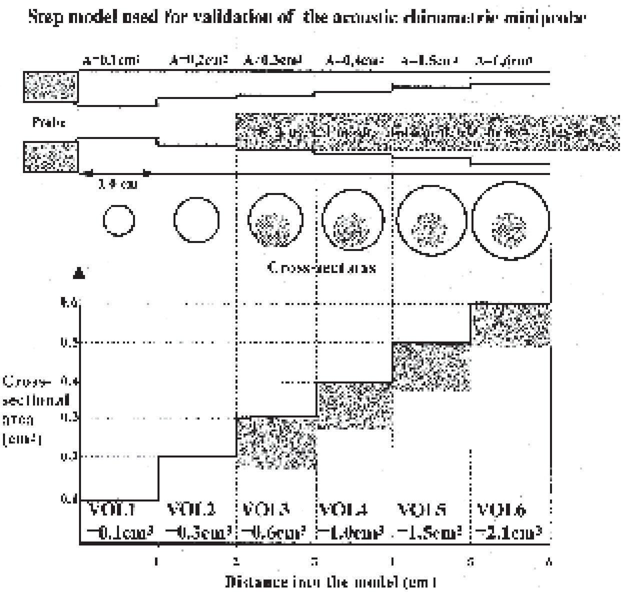

Figure 1. Line drawing illustrating the shape and configuration of the step model used for validation of the miniprobe. The cross-sectional areas and the volumes at different depths into the standardised model are listed. The position and effect of the rods inserted on the dimensions and shape of the cross-sectional area are illustrated by the shaded areas.

The influence of time and external factors like temperature, pressure and noise on the reproducibility of the acoustic measurements was evaluated in a standardised tubular model with dimensions increasing from 0.1 cm^2 to 0.6 cm^2 in one centimetre long steps (Fig 1) . Following calibration at 17°C, the digitally monitored temperature was slowly increased from 17-25°C and acoustic measurements were performed at 1.0°C steps.
In a second series, calibration was repeated and measurements again performed at each °C from 17-25°C . Humidity varied between 60% to 68% with a tendency to augment with increasing temperature. The effect of pressure changes on the acoustic curves was examined by simulating tidal respiration of neonates (Tidal volume≈25ml, Respiratory rate≈50, Peak flow≈60ml/s (Lodrup et al., 1992)) through parallel models with MCA´s of 0.1cm^2. The pressure changes induced (measured by a manometer) were similar to those reported by Solow and Peitersen during anterior rhinomanometry (≈+/-100-150 dPa) (Solow and Peitersen, 1991). The influence of external noise was evaluated by exposing the probe during measurements in the step-model to a range of wide-band noise of intensities from 45 dB SPL (background noise level) to 74 dB SPL measured at a distance of 10 cm from the probe. A gradual constriction, resembling the actual shape found at the internal isthmus, was created by inverting two identical discs with MCA ranging from 0.02-0.08 cm^2. Rods with known CA, length and volume were introduced into the standard step model to simulate the concha inferior and the narrow slit-like configuration it creates (Fig. 1).

CALCULATIONS AND STATISTICS

Repeatability is defined as the closeness of agreement between successive measurements of the same model carried out by the same person, the same method, the same instrument, same probe the same location, same ambient conditions and repeated over a short period of time. *Reproducibility* is defined as the closeness of agreement of the results when individual measurements are carried out under changing conditions such as time, temperature, pressure, calibration sequence and probe. *Accuracy* is defined as the agreement between the results of the measured acoustic curve and the true value of the model.
For every model we recorded five curves, (9 in the pressure and noise series) and computed the mean values, standard deviation (SD) , coefficient of variation (CV=SD/mean) and its percentage of the mean (CV%). The data obtained from the examinations were stored in the rhinometer hard disk and transferred to

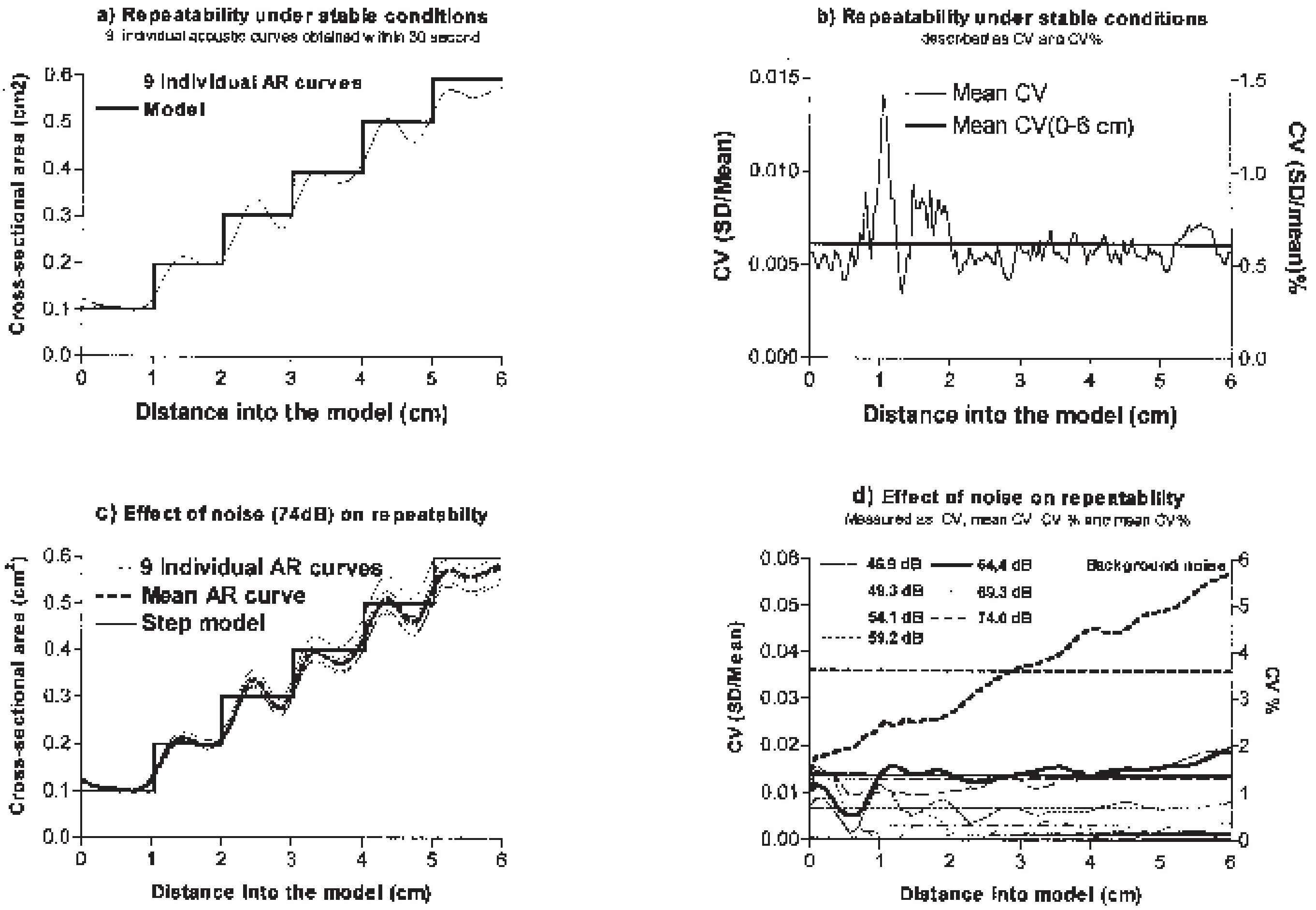

Figure 2. Figure 2a show a typical rhinogram containing 9 individual rhinometric curves. The mean repeatability of the rhinometric series of 5 individual rhinometric curves obtained seconds apart, but at different times of the day, different temperatures and with different probes is shown in figure 2b. Nine individual acoustic curves obtained during exposure to 74 dB SPL are shown in figure 2c. The effect on repeatability of external noise levels, increasing in 5dB steps, from background noise (≈45dB) to a noise level of 74 dBSPL, is shown in figure 2d.

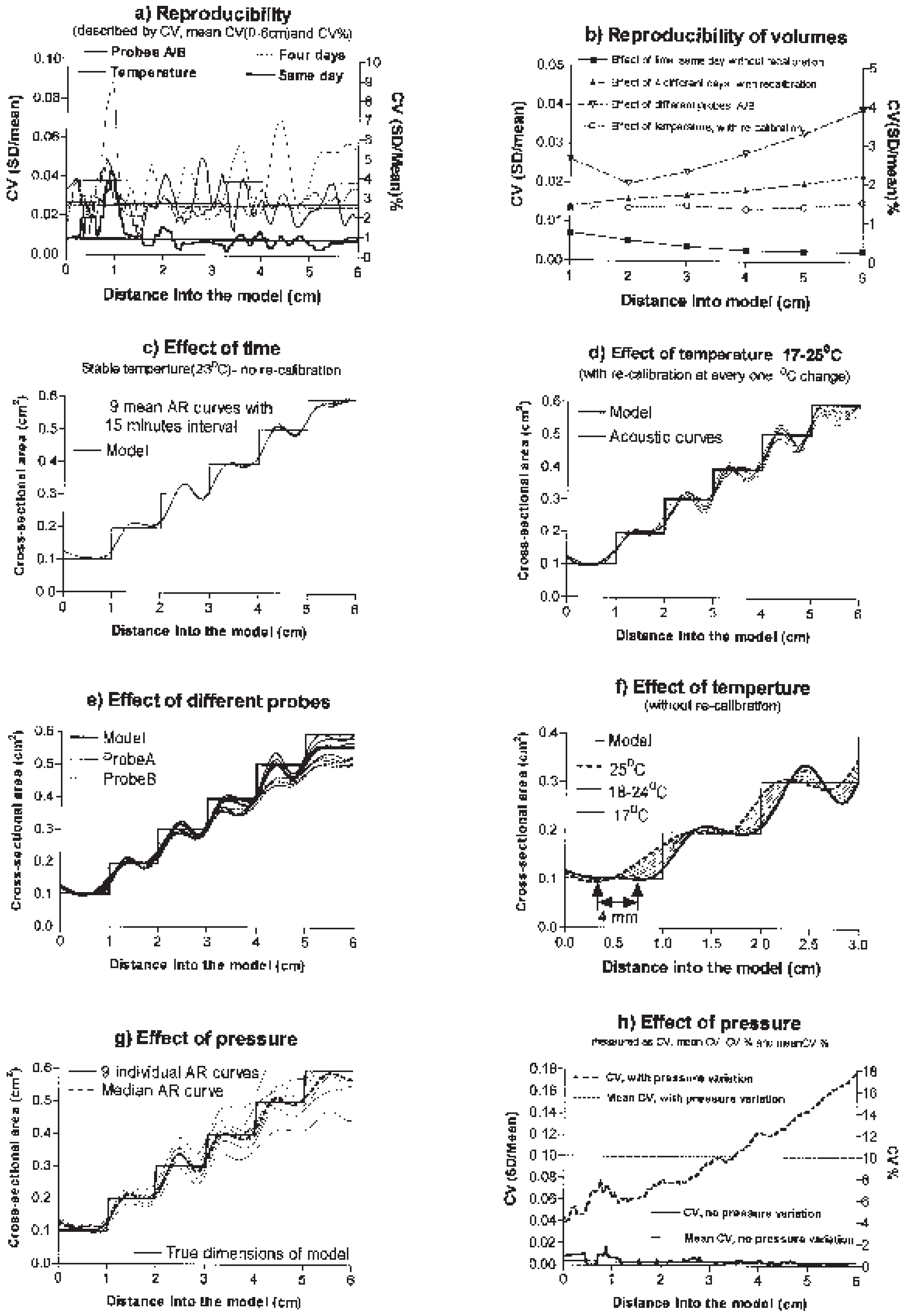

Figure 3. The reproducibility of the cross-sectional areas and volumes at different depths into the standard step model expressed as the CV and the CV% with variation in time, temperature and probes are shown in figures 3a and 3b respectively. The corresponding acoustic curves are shown in figures 3c-e. The effect of increasing the temperature from 17-25°C without re-calibration is shown in figure 3f. The acoustic curves obtained during different phases of the respiratory cycle are shown in figure 3g, and the effect of pressure variation on reproducibility during simulated respiration is shown in figure 3h.

Excel 4.0 for data management. Statistical analysis and presentation were performed using SAS 6.08 and PRISM Graph Pad 2.01. Repeatability was examined from the five curves (9 for noise and pressure) in each of 30 files. Reproducibility was calculated for the different series with changing factors such as probe, temperature and time and expressed as CV and CV %. Accuracy of the MCA, its position (DMCA) and volumes at different distances into the model (VOL1-VOL6) were estimated from a selection of the same series of measurements and expressed as the difference (% error) between the mean rhinometric curve and the true dimensions of the model.

RESULTS

Repeatability

An example of acoustic measurements performed in the standard step model under stable ambient conditions is shown in figure 2a. The mean repeatability of the five successive acoustic curves obtained seconds apart at different times of the day, different temperature and with different probes is shown in figure 2b. The mean SD was 0.0012 and the mean CV was 0.6% and never larger than 1.5% (Fig. 2b). When the model was exposed to constant noise levels higher than 60 dB the mean CV increased (Fig. 2c) and reached 3.5% for 74 dB (Fig. 2d).

Reproducibility

The mean reproducibility of measurements performed during the same day without and with re-calibration between measurements was excellent (CV<1%) (Figs.3a,b,c). The mean reproducibility of measurements performed on four different days was high (CV%<3%) (Figs. 3a,b). The effect of changes in temperature measured as the mean CV% was also less than 3% (Figs. 3a,b,d) provided re-calibration was performed, whereas the effect of changing probes was slightly greater (CV%<4%) (Fig. 3a,b,e). Fast pressure changes induced by simulating respiration further decreased the reproducibility (CV%=10%) (Figs. 3g,h). If re-calibration was not performed with increasing temperature, the position of the MCA (DMCA) moved further into the model by approximately 0.4 mm/°C (Fig. 3f). The reproducibility of the volumes of the model at 1.0 cm steps into the model calculated as CV% for the effect of time, temperature, and changing probes never exceeded 4% (Fig.3b) and the corresponding CV% for the MCA in the step model (MCA=0.1 cm^2) was <2.5%. The reproducibility of the DMCA, evaluated in the models with distinctly positioned MCA´s shown in figures 4a, 4b and 5a, was CV%<8% (SD<0.04 cm) at the position 0.5 cm from the entrance of the model.

Accuracy

In general, the ability to correctly determine the absolute value of the MCA was high with a maximum error of 0.003 cm^2 when MCA was 0.1 cm^2 (%error<3%), regardless of changes in time temperature and probes as illustrated by figures 3c,d,e. The error in determination of MCA with decreasing values of MCA was less than 12% for MCA of 0.05 cm^2 and larger (Figs. 4a-e) and the absolute value never exceeded 0.012 cm^2 even when MCA was as small as 0.02 cm^2 (Figs. 4d,e). The DMCA was determined with high accuracy regardless of its position and size of the MCA (MCA=0.02-1.0 cm^2) (Figs. 4d). The absolute error never exceeded 0.6 mm and the % error was less than ±12% even when the MCA was located as far anteriorly as 0,5 cm from the model entrance (Fig. 4d). There was no systematic lag of the rhinometric curves (Figs. 4a,b,d). The accuracy of the CA´s along the X-axis and different volumes from the entrance to different distances into the step model (model A) are shown in figures 4c and 4g respectively. The ability to accurately determine the posterior volume (VOL4), used as a clinical parameter, was, however, acceptable (% error <10%, absolute error<0.04cm^3) if the CA of the cavity posterior to the MCA did not exceed the MCA by a factor of 3-4 as seen in different models A-E (Fig. 4 a,b,f). The error in the determination of the volume between 2 and 4 cm was less than 10% even when the CA between 1 and 2 cm is largely underestimated (in model D) (Fig. 4a). The shape of the CA in the model with rods inserted to simulate the concha is illustrated in figures 1 and 5a. The accuracy of the volumes derived from measurements with rods of different dimensions inserted into the standard model is maintained regardless of the more complex configuration (Fig. 5b). In accordance with the result from the tubular models, the accuracy of the MCA (Figs. 4c,d) as well as the determination of volumes of the posterior cavity (Figs. 4a,b,f) declined considerably when the MCA became very small (Figs. 5a,b).

If the entrance dimensions of the model exceed the probe dimensions by a factor of 2-3, accuracy of the cavity both anterior and posterior to the MCA decreases, whereas the determinations of the MCA itself remain accurate (Fig. 6a). Figure 6b indicates that if the width of the constriction is smaller than the SR (≈0.38 cm), the accuracy decreases and twin constrictions are not separated if the distance between them is less than the SR (Fig. 6c). Change in position of the MCA within the anterior 2 cm of the cavity seems to have only minor influence on the accuracy of the posterior measurements (Fig. 6d).

The 9 individual curves obtained randomly in different phases of the simulated pressure changes during respiration (Figs. 3g+h), as well as the curves obtained under influence of external noise (Figs. 2c+d), vary between over- and underestimation. Consequently, despite a considerably reduced repeatability and reproducibility, the accuracy of the mean curves obtained during constant noise exposure and pressure variations during simulated respiration respectively, remained acceptable (% error VOL4 <5%), provided a sufficient number of randomly recorded curves was analysed (Figs. 2c,d, 3g,h).

DISCUSSION

The repeatability of the measurements is excellent (CV<0.6%) (Fig.2). The mean reproducibility of the anterior 6 cm is in general high (CV%<4%) provided the ambient conditions remain relatively stable (Fig. 3). The determination of the parameters used in clinical work (Djupesland and Lyholm, 1997), MCA, DMCA and VOL4 is accurate provided the MCA and its dimensions relative to the posterior cavity remain within limits largely determined by the inherent properties of the probe in question (Figs. 4,5).

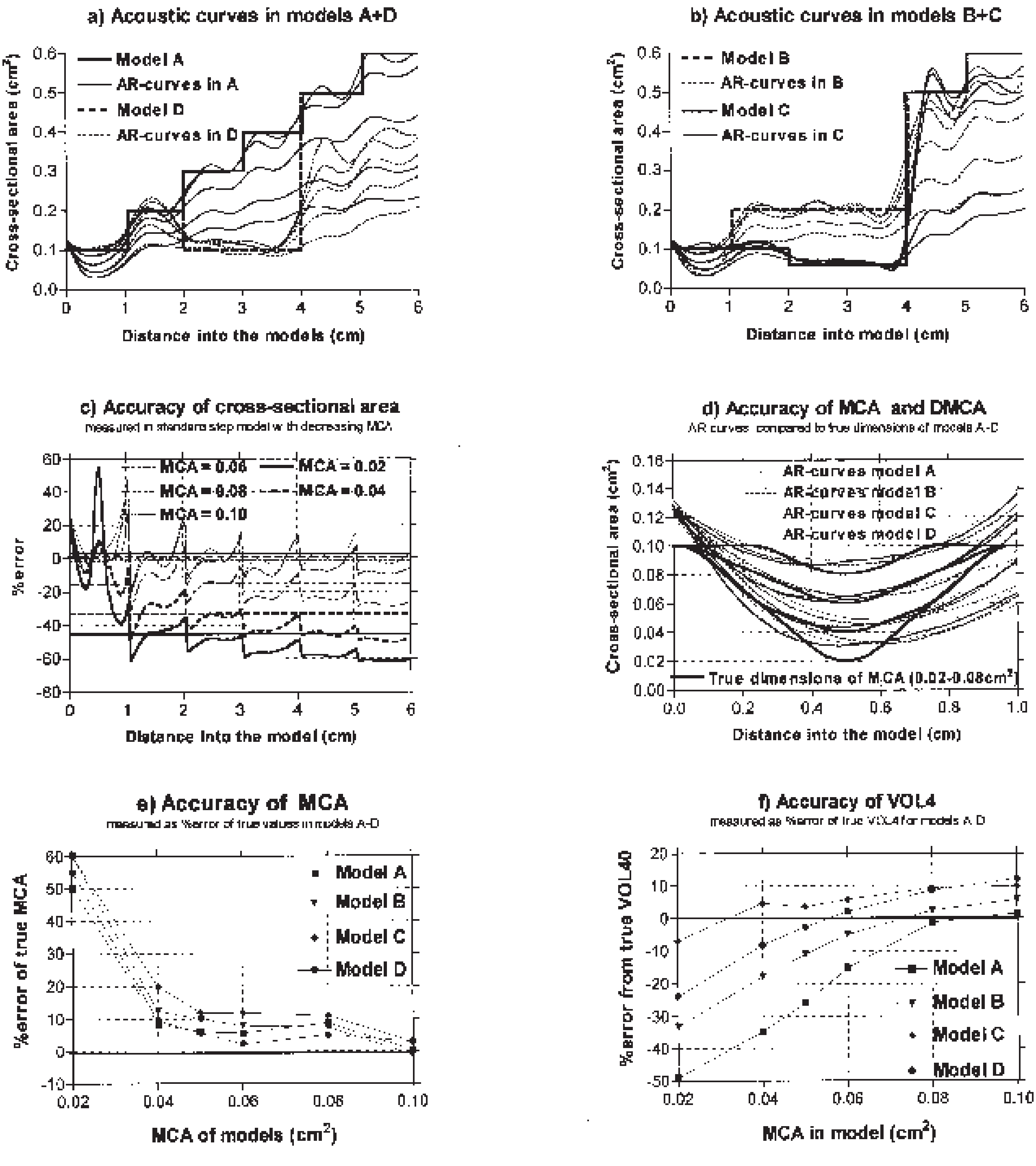

Figure 4. The true dimensions of the different models A-D with MCA varying from 0.1-0.02cm^2 and the corresponding acoustic curves are shown in figure 4a and 4b. The accuracy of the cross-sectional areas at any point along the x-axis in model A and the mean accuracy of the anterior 6 cm, with decreasing MCA is shown in figure 4c. The details of the model and the acoustic curves of the anterior 10 mm of the models A-D are shown in figure 4d. The error expressed as percentage deviation (% error) from the true dimensions of the model values is shown for MCA in figure 4e. The accuracy of VOL4 for the models A-D (see figs. 4a+b) with MCA decreasing from 0.1 cm^2 to 0.02 cm^2 is shown in figure 4f.

Impedance matching

Although the smaller dimensions of the nasal airway reduce the theoretical bandwidth restrictions considerably (Djupesland and Lyholm, 1997; Hilberg et al., 1989; Fredberg et al., 1980; Jackson et al., 1977), the anteriorly located narrow nasal valve may severely reduce accuracy of the posterior measurements due to violation of the basic assumption of negligible viscous energy loss (Hilberg et al., 1989; Marchall, 1992). Our results concur with previous studies suggesting reduced ability to estimate the posterior dimensions when the anterior constriction

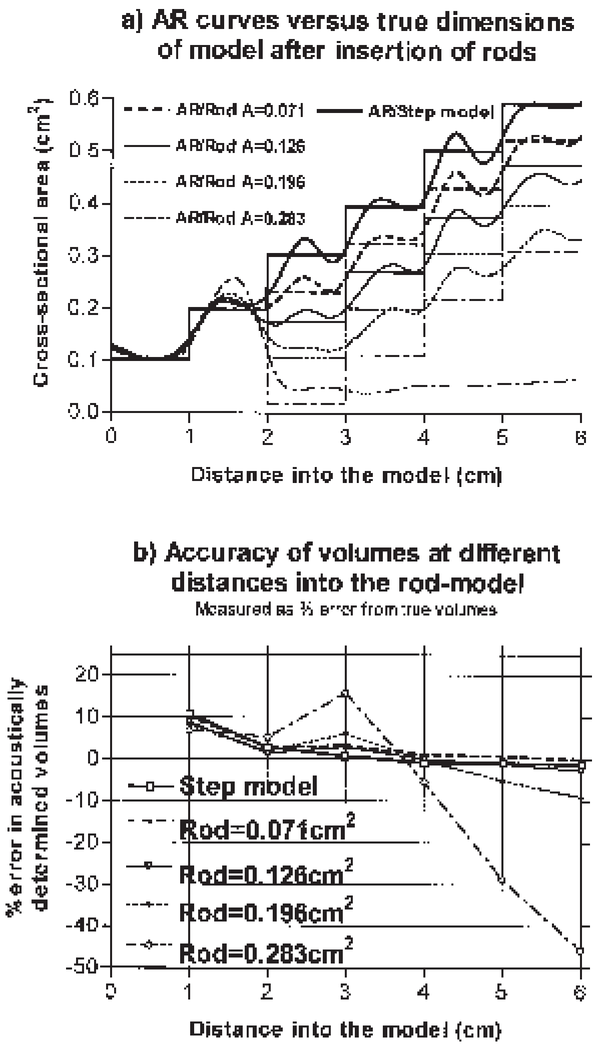

Figure 5. The true CA′s of the different models with the rods inserted and the corresponding mean acoustic curves are shown in figure 5a. The accuracy of the volumes with the different rods in the model expressed as % error is shown in figure 5b.

becomes less than 30-40 % of the internal cross-sectional area of the probe (Hilberg et al., 1989; Marchall, 1992) (Figs. 4,5). Consequently, the CA of the commercial rhinometer probes, ranging from 1.2 - 2.1 cm^2 seems larger than that which is optimal even for adults (Hilberg et al., 1989; Lenders et al., 1992; Buenting et al., 1994; Pedersen et al., 1994; Kano et al., 1994; Cole and Roithmann, 1996; Roithmann et al., 1995; Zavras et al., 1994; Riechelmann et al., 1993). When such probes are applied to infants and children (Buenting et al., 1994; Riechelmann et al., 1993; Pedersen et al., 1994; Kano et al., 1994; Zavras et al., 1994) and to models with infant dimensions (Buenting et al., 1994), artefacts are more likely to occur. Modification of the probes reducing the internal diameter (Riechelmann et al., 1993; Buenting et al., 1994) and the use of conical nose pieces may reduce the dimensional mismatch. Poor impedance matching, however, probably explains the overestimation of narrow apertures and the lag of the curves observed in the models used for validation in many studies (Jackson et al., 1977; Pedersen et al., 1994; Kano et al., 1994; Lenders et al., 1992; Riechelmann et al., 1993; Buenting et al., 1994). The dimensions (CA=0.12 cm^2) and the frequency bandwidth (125Hz-20kHz) of the miniprobe were chosen to obtain optimal impedance matching between the probe and the nostril and at the same time achieve the maximum resolution of the MCA as well as the posterior part of the nasal cavity (Djupesland and Lyholm, 1997). In addition, the wider bandwidth of the infant probe (Djupesland and Lyholm, 1997) reduces the potential error induced by the non-rigid behaviour of the nasal mucosa for frequencies less than 1000Hz (Hilberg et al., 1998; Hilberg et al., 1989; Marchall, 1992).

Limits of accuracy

Figure 6a shows that as long as the anterior aperture remains below approximately 0.4 cm^2 , a MCA of 0.1 cm^2 is still accurately determined, whereas the accuracy of the measurements posterior to the MCA declines, underlining the importance of impedance matching between the probe and the dimensions of the nasal inlet. The MCA is determined with acceptable accuracy (error$<$ 12%) provided it is greater than 0.04 cm^2 (Figs. 4c,d), which is in fact the lower value found in healthy infants (Djupesland and Lyholm, 1997). Below this MCA, accuracy declines and the MCA tends to be overestimated, in accordance with previous studies (Marchall, 1992; Hilberg et al., 1989) (Figs. 4d,e). Due to the very small dimensions in question, the deviation expressed as a percentage of the MCA becomes large, although the absolute value never exceeded 0.012 cm^2 (Fig 4d,e). If the length of the constriction becomes less than the SR the ability to determine MCA accurately declines (Jackson et al., 1977; Hamilton et al., 1995; Buenting et al., 1994) (Fig.6b). Variations in position within the anterior 2 cm have only minor impact on the accuracy of the MCA (Fig. 6d), but two MCA′s are, of course, not separated from each other if the distance between them is less than the SR (Fig. 6c). From the series of AR measurements a fairly regular pattern emerges, indicating that the ability to correctly determine the volume posterior to the MCA gradually declines when the dimensions immediately posterior exceed the MCA by a factor of 3-4 (Fig. 4). Although no specific figures have been reported, inspection of the illustrations provided in previous studies suggests a similar relationship (Buenting et al., 1994; Hamilton et al., 1995; Jackson et al., 1977; Hilberg et al., 1993; Hilberg et al., 1989).

At birth, the MCA is located corresponding to the isthmus (Pedersen et al., 1994; Buenting et al., 1994; Djupesland and Lyholm, 1997) and the shape is triangular or oval. Further posteriorly the configuration becomes more complex due to the turbinates. The result of measurements in the models with rods inserted (Fig.1) clearly indicates that the CA is accurately determined regardless of its configuration (Fig. 5). This confirms findings in previous studies with CT/MRI imaging, water displacement of casts and cadavers (Buenting et al., 1994; Hilberg et al., 1993; Hilberg et al., 1989), and is essential to the validity of AR in clinical practice. The anatomical studies of Wolf based on CT scans and dissection of cadavers of 38 infants show that the shape of the choanal aperture is close to circular with a

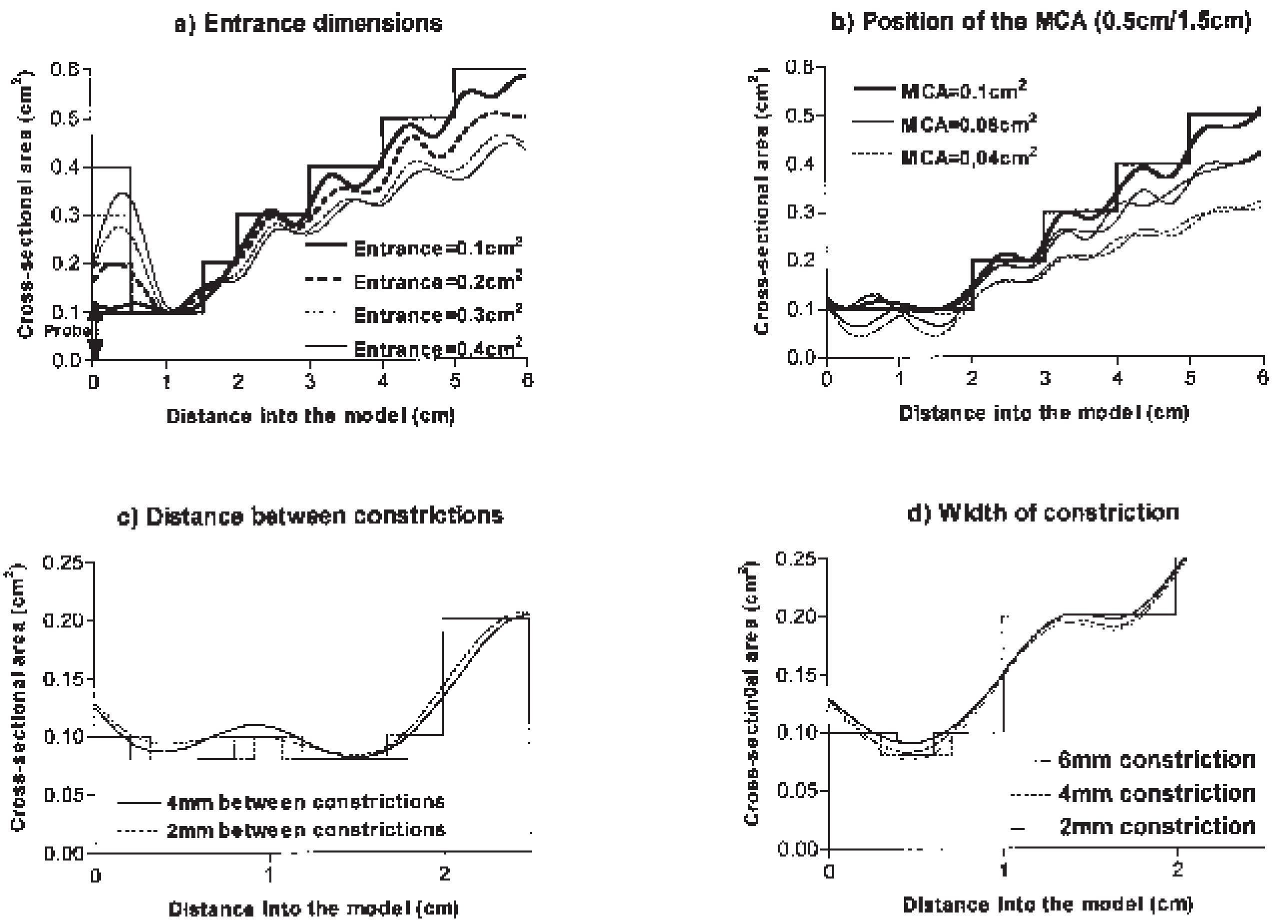

Figure 6. The effect of increasing dimensions at the entrance of the model (corresponding to increasing size of the nostril) is shown in figure 6a. The effect of changing width of the MCA on posterior measurements is shown in figure 6b. The ability to separate two constrictions is illustrated in figure 6c, and the effect of changing position of the constriction is shown in figure 6d.

mean diameter of 6 mm corresponding to an area of approximately 0.3 cm^2 (Wolf et al., 1993). This value is strikingly similar to the mean acoustic values of ≈0.3 cm^2 and ≈0.35 cm^2 at the transition to the epipharynx in neonates (Pedersen et al., 1994; Buenting et al., 1994; Djupesland and Lyholm, 1997) and one year old infants respectively (Djupesland, unpublished). Hence, the CA at the choanal aperture normally seems to be well within the empirical limit of 3-4 times the MCA which is 0.1 cm^2 at birth (Pedersen et al., 1994; Buenting et al., 1994; Djupesland and Lyholm, 1997)and 0.17 cm^2 at one year of age (Djupesland, submitted data).

The influence of growth and infection

As the child grows and inevitably experiences infections, a second constriction with location corresponding to the head of the inferior turbinate becomes more evident(Riechelmann et al., 1993; Djupesland, unpublished), which is the location of MCA in most adults (Cole and Roithmann, 1996; Roithmann et al., 1995; Hilberg et al., 1989). This change in geometry appears to be the combined result of growth and mucosal swelling due to infection or allergy. Fortunately, the dimensions posterior to the MCA are normally more markedly reduced than the MCA itself (Kano et al., 1994; Djupesland, unpublished), thus maintaining or improving the acoustic resolution of the cavity posterior to the MCA. The present and previous results from infants and children seriously challenge the recent suggestion by Hamilton et al. that the MCA1 merely represents an artefact due to the nosepiece rather that a true anatomic structure (Hamilton et al., 1997).

The shape of the cross-sectional areas posterior to the head of the inferior turbinate, particularly in response to inflammatory mucosal swelling, becomes increasingly narrow and slit-like as compared to the oval or triangular shaped anterior constriction. The increasing complexity of the conduit will have important consequences for the aerodynamic properties (Hey and Price, 1982) that need further elucidation.

Variation in temperature, pressure, external noise and probes

When the temperature rises and the speed of sound increases, the reflections consequently arrive earlier, explaining the shift of the curve (i.e. position of the MCA) (Fig. 3f) to the left of approximately 0.4 mm for each degree centigrade. This figure is in close agreement with the recently reported result of Tomkinson and Eccles, 1996. As illustrated by figures 3d and 3f, the reproducibility of the acoustic curves is improved when re-calibration is performed before measurements at each new temperature level. It is thus recommended to monitor the temperature during measurements over time. Tomkinson has also pointed out the potential error induced by the pressure changes induced by respiration which may influence the properties of the microphone recording the reflections (Tomkinson and Eccles, 1995) (Figs.3g,h). In infants and small children neither able nor willing to co-operate this may represent an important source of error. However, in our experience with the miniprobe this does not represent a major problem, primarily because most infants take a brief pause in respiration in response to the tactile stimulation when applying the probe. Due to the opposite effect of error induced by inspiration and expiration, accuracy remains acceptable (% error VOL4<4%) if a sufficiently high number of curves is recorded randomly in different phases of respiration (Fig. 3g).

As long as the external noise level was less than 60 dB SPL the repeatability remained unchanged (Fig. 2d). In the discussion of noise-induced artefacts it is, however, important to emphasise that the frequency content of the noise plays a significant role. The mathematical nature of the area reconstruction algorithm (Ware-Aki) has the characteristics of an integrating function. Therefore, noise-induced errors are accumulated throughout the area-distance function if the errors have the same sign, (low frequency noise), resulting in a constantly increasing total error. On the other hand, noise with fast changing sign (+/–) (i.e. high frequency noise), tends to be eliminated, this being illustrated by the maintained accuracy (%error<4%) despite reduced repeatability of the mean curve if a high number of curves is recorded (Fig. 2c). In practice, it is particularly important to avoid noise disturbances during calibration because systematic error of the subsequent measurements may result. Noise artefacts during measurements are usually evidenced by sudden distortion of the curves, thus making detection and rejection easy.

During calibration of the infant probes, a spectrum equaliser adjusts the incident digital signal to the properties of the microphone of the probe, which explains the observed difference in measurements between probes. Consequently, slight variations in the properties between microphones may induce differences in the frequency spectrum and intensity of the incident signal. The reproducibility of the volumes obtained with the different probes declines with increasing distance from the probe, but remains acceptable as long as the increase of CA does not exceed the value of the MCA by a factor of 3-4 (Figs. 3a,b,e).

It is essential to remember that improved and well defined technical properties are of little value if other sources of error, such as incomplete coupling between the nosepiece and the nostril, are not avoided. Inappropriate use of the technique and misleading interpretations of the results will discredit the method and its potential role as a reliable tool in research and clinical rhinology. Standardisation of both the validation and operating procedures is urgently needed.

CONCLUSIONS AND RECOMMENDATIONS

The dimensions of the probe and nosepiece should be optimised to match the size of the nostril, but at the same time should not exceed approximately 40% of the lower normal range of MCA in the age group in question.

The maximum bandwidth frequency of rhinometric probes should be optimised to allow determination of the upper normal range (mean +2SD) of the dimensions at the choanal aperture in the age group in question.

Validation procedures should include calibration in a standardised step model allowing visual inspection of the results, and the curve should be stored to provide documentation.

Alarm functions should be implemented in the software giving warning if the recommended range of dimensions is violated.

Temperature in the probe at calibration should be monitored and re-calibration should be performed, if the temperature changes by more than 2-3 0C.

Pressure sensors implemented in the probes could reduce pressure induced artefacts. Open probes should be considered.

ACKNOWLEDGEMENTS

The authors are grateful to Professor I.W.S Mair for his critical revision of the manuscript and to audio-physicist Arne Sundby, and audio-engineer Anders Blix for their assistance in the evaluation of the influence of external noise on the acoustic measurements.

This study was supported by grants from the Norwegian Research Council, the Norwegian Health Association and the Norwegian Asthma and Allergy Foundation.

LIST OF ABBREVIATIONS

AD	=	area-distance relationship
AR	=	acoustic rhinometry
dB	=	decibel
CA	=	cross-sectional area
c_0	=	speed of sound in air
CV	=	coefficient of variation (SD/mean)
CV%	=	coefficient of variation as % of mean
DMCA	=	distance from entrance to the MCA
d_{max}	=	maximum diameter
f_{max}	=	maximum frequency
f_s	=	sampling frequency
MCA	=	minimum cross-sectional area
SR	=	spatial resolution
SD	=	standard deviation
SPL	=	sound pressure level
VOL4	=	volume of anterior 4 cm

REFERENCES

1. Buenting JE, Dalston RM, Drake AF (1994) Nasal cavity area in term infants determined by acoustic rhinometry. Laryngoscope 104: 1439-1445.
2. Buenting JE, Dalston RM, Smith TL, Drake AF (1994) Artifacts associated with acoustic Rhinometric assessment of infants and young children: a model study. J Appl Physiol 77: 2558-2563.
3. Cole P, Roithmann R (1996) The nasal valve and current technology. Am J Rhinol 10: 23-31.
4. Djupesland PG, Kaastad E, Franzén G (1997) Acoustic rhinometry in the evaluation of congenital choanal malformations. Int J Pediatr Otorhinolaryngol 41: 319-337.

5. Djupesland PG, Lodrup Carlsen KC (1997) Nasal airway dimensions and lung function in healthy, awake neonates. Pediatr Pulmonol ?: 99-106.
6. Djupesland PG, Lyholm B (1997) Nasal airway dimensions in term neonates measured by continuous wide-band noise acoustic rhinometry. Acta Otolaryngol (Stockh) 117: 424-432.
7. Fisher EW, Boreham AB (1995) Improving the reproducibility of acoustic rhinometry: a customized stand giving control of height and angle. J Laryngol Otol 109: 536-537.
8. Fisher EW, Morris DP, Biemans JM, Palmer CR, Lund, VJ (1995) Practical aspects of acoustic rhinometry: problems and solutions. Rhinology 33: 219-223.
9. Fredberg JJ, Wohl ME, Glass GM, Dorkin HL (1980) Airway area by acoustic reflections measured at the mouth. J Appl Physiol 48: 749-758.
10. Hamilton JW, Cook JA, Phillips DE, Jones AS (1995) Limitations of acoustic rhinometry determined by a simple model. Acta Otolaryngol (Stockh) 115: 811-814.
11. Hamilton JW, McRae RD, Jones AS (1997) The magnitude of random errors in acoustic rhinometry and re-interpretation of the acoustic profile. Clin Otolaryngol 22: 408-413.
12. Hamilton JW, McRae RD, Phillips DE, Jones AS (1995) The accuracy of acoustic rhinometry using a pulse train signal. Clin Otolaryngol 20: 279-282.
13. Hey EN, Price JF (1982) Nasal conductance and effective airway diameter. J Physiol (Lond) 330: 429-437.
14. Hilberg O, Jackson AC, Swift DL, Pedersen OF (1989) Acoustic rhinometry: evaluation of nasal cavity geometry by acoustic reflection. J Appl Physiol 66: 295-303.
15. Hilberg O, Jensen FT, Pedersen OF (1993) Nasal airway geometry: comparison between acoustic reflections and magnetic resonans scanning. J Appl Physiol 75: 2811-2819.
16. Hilberg O, Lyholm B, Michelsen A, Pedersen B, Jackson O (1998) Acoustic reflections during rhinometry: spatial resolution and sound loss. J Appl Physiol 84: 1030-1039.
17. Hilberg O, Pedersen OF (1996) Acoustic rhinometry: influence of paranasal sinuses. J Appl Physiol 80: 1589-1594.
18. Hoffstein V, Fredberg JJ (1991) The acoustic reflection technique for non-invasive assessment of upper airway area. [Review]. Eur Respir J 4: 602-611.
19. Jackson AC, Butler J, Millet EJ, Hoppin FG, Dawson SV (1977) Airway geometry by analysis of acoustic pulse response measurements. J Appl Physiol ?: 523-536.
20. Kano S, Pedersen OF, Sly PD (1994) Nasal response to inhaled histamine measured by acoustic rhinometry in infants. Pediatr Pulmonol 17: 312-319.
21. Lenders H, Scholl R, Brunner M (1992) [Acoustic rhinometry: the bat principle of the nose]. [German]. HNO 40: 239-247.
22. Lodrup KC, Mowinckel P, Carlsen KH (1992) Lung function measurements in awake compared to sleeping newborn infants. Pediatr Pulmonol 12: 99-104.
23. Marchall I (1992) Impedance reconstruction methods for pulse reflectrometry. Acustica 76: 118-128.
24. Molfino N, Zamel N, Hoffstein V, Fredberg J (1990) Artifacts in measuring airway areas by acoustic reflections. Am Rev Respir Dis 142: 1465-1466.
25. Pedersen OF, Berkowitz R, Yamagiwa M, and Hilberg O (1994) Nasal cavity dimensions in the newborn measured by acoustic reflections. Laryngoscope 104: 1023-1028.
26. Riechelmann H, Reinheimer M, Wolfensberger M (1993) Acoustic rhinometry in pre-school children. Clin Otolaryngol ?: 272-277.
27. Rivlin J, Hoffstein V, Kalbfleisch J, McNicholas W, Zamel N, Bryan, A (1984) Upper airway morphology in patients with idiopathic obstructive sleep apnea. Am Rev Respir Dis 129: 355-360.
28. Roithmann R, Cole P, Chapnik J, Shpirer I, Hoffstein V, Zamel N (1995) Acoustic rhinometry in the evaluation of nasal obstruction. Laryngoscope 105: 275-281.
29. Solow B, Peitersen B (1991) Nasal airway resistance in the newborn. Rhinology 29: 27-33.
30. Sondhi MM, Gopinath B (1970) Determination of vocal-tract shape from impulse response at the lips. J Acoust Soc Am 36: 1867-1873.
31. Tomkinson A (1995) The reliability of acoustic rhinometry. J Laryngol Otol 109: 1234
32. Tomkinson A (1997) Acoustic rhinometry: its place in rhinology (Editorial). Clin Otolaryngol 22: 189-191.
33. Tomkinson A, Eccles R (1995) Errors arising in cross-sectional area estimation by acoustic rhinometry produced by breathing during measurement. Rhinology 33: 138-140.
34. Tomkinson A, and Eccles R (1996) The effect of changes in ambient temperature on the reliability of acoustic rhinometry data. Rhinology 34: 75-77.
35. Wolf G, Anderhuber W, Kuhn F (1993) Development of the paranasal sinuses in children: implications for paranasal sinus surgery. [Review] Ann Otol. Rhinol Laryngol 102: 705-711.
36. Zavras AI, White GE, Rich A, Jackson AC (1994) Acoustic rhinometry in the evaluation of children with nasal or oral respiration. J Clin Pediatr Dent 18: 203-210.

Per Djupesland, M.D.
Department of Otorhinolaryngology
Ullevaal University Hospital
0407 Oslo
Norway
Tel: +47-22118570
Fax:+47-22118555
E-mail: per.djupesland@ioks.uio.no